

dio astronomy, and plasma waves investigations for discussions of these early results. We also thank J. A. Van Allen for comments on these results. We thank the entire Voyager Project staff at JPL for the success of the mission and their support of our investigation, especially G. Sisk, E. Franzgrote, N. Toy, H. Woo, O. Divers, and W. McDougal. For

support at GSFC we thank W. Mish and his data-processing and analysis team, particularly T. Vollmer, R. Kennan, P. Hodge, P. Harrison, J. Jones, T. Carleton, J. Annen, G. Burgess, J. Byrnes, S. Kempler, L. Moriarty, F. Ottens, A. Silver, and R. Thompson; C. Moyer, J. Scheifele, J. Seck, and E. Worley for contributions to the design, develop-

ment, and testing of the hardware; and F. Hunsaker and S. Myers for graphics support. F.M.N. was supported financially by the German Ministry of Science and Technology. N.F.N. was supported in part by JPL contract 957921.

25 October 1989; accepted 15 November 1989

Plasma Observations Near Neptune: Initial Results from Voyager 2

J. W. BELCHER, H. S. BRIDGE, F. BAGENAL, B. COPPI, O. DIVERS, A. EVIATAR, G. S. GORDON, JR., A. J. LAZARUS, R. L. MCNUTT, JR., K. W. OGILVIE, J. D. RICHARDSON, G. L. SISCOE, E. C. SITTLER, JR., J. T. STEINBERG, J. D. SULLIVAN, A. SZABO, L. VILLANUEVA, V. M. VASYLIUNAS, M. ZHANG

The plasma science experiment on Voyager 2 made observations of the plasma environment in Neptune's magnetosphere and in the surrounding solar wind. Because of the large tilt of the magnetic dipole and fortuitous timing, Voyager entered Neptune's magnetosphere through the cusp region, the first cusp observations at an outer planet. Thus the transition from the magnetosheath to the magnetosphere observed by Voyager 2 was not sharp but rather appeared as a gradual decrease in plasma density and temperature. The maximum plasma density observed in the magnetosphere is inferred to be 1.4 per cubic centimeter (the exact value depends on the composition), the smallest observed by Voyager in any magnetosphere. The plasma has at least two components; light ions (mass, 1 to 5) and heavy ions (mass, 10 to 40), but more precise species identification is not yet available. Most of the plasma is concentrated in a plasma sheet or plasma torus and near closest approach to the planet. A likely source of the heavy ions is Triton's atmosphere or ionosphere, whereas the light ions probably escape from Neptune. The large tilt of Neptune's magnetic dipole produces a dynamic magnetosphere that changes configuration every 16 hours as the planet rotates.

NEPTUNE'S MAGNETOSPHERE IS the last to be visited by a Voyager spacecraft. As at Uranus, the very existence of a magnetosphere at Neptune was in question until the Voyager 2 flyby. This encounter was unique since Voyager approached much closer to Neptune, 1.2 Neptunian radii ($1 R_N = 24,765$ km), than it had to any other planet and also made the first pass over the rotational pole of a giant planet. In this report we describe observations of the spatial distribution and physical properties of the plasma near Neptune.

The Voyager plasma science (PLS) experiment measured positive ions and electrons with energies per charge from 10 to 5950 V (1). These observations were obtained simultaneously in four modulated-grid Faraday cup detectors. Three of these detectors (A, B, and C sensors) pointed approximately toward Earth and were ideally oriented for measuring solar wind and magnetosheath plasma. The D sensor "looked" at right angles to this direction and was oriented via spacecraft rolls to look into the corotation direction (toward plasma moving azimuthally in the direction of Neptune's rotation) inbound and outbound from the planet and upward (away from the planet) near closest approach. Four different measurement modes were used. A high-resolution M mode ($\Delta E/E = 3.6\%$) and a low-resolution L mode ($\Delta E/E = 29\%$) measure ion currents over the entire energy-per-charge range of the instrument (10 to 5950 V). A high-energy E2 mode (140 to 5950 eV) and low-energy E1 mode (10 to 140 eV) measure electron currents with energy resolutions $\Delta E/E$ of 29 and 9.9%,

respectively. The nominal time resolution of the data shown here is 48 s for ion data and 96 s for electron data.

Figure 1 shows an overview of the plasma measurements near Neptune, including the ion currents measured in the C sensor, electron currents, and electron densities measured along the spacecraft trajectory, which is shown in Fig. 2. The currents plotted are summations over energy per charge from 10 to 140 V for electrons and 10 to 1000 V for ions. The analysis used to compute the electron density profile is similar to that used at Uranus (2) except that, because of the low fluxes at higher energies, only E1 spectra were used.

Bow shock and magnetopause. The bow shock and magnetopause crossings are labeled in Fig. 1. A list of crossing times is given in Table 1, and the locations of these crossings on the spacecraft trajectory are indicated in Fig. 2. Multiple crossings may have occurred outbound, leading to some uncertainty in the quoted times. In general, these crossing times agree fairly well with identifications made by means of the magnetometry (MAG) data (3). Upstream of the bow shock the solar wind protons were moving as a cold beam with a streaming energy of 850 eV. On crossing the shock, the ions slowed down and were heated to several hundred electron volts. The total flux of ions remained roughly constant across the shock and into the magnetosheath. Electrons, which were too cold to be observed by the PLS instrument in the solar wind, were heated at the shock and were detected in the low-energy electron channels in the magnetosheath. The model curves in Fig. 2 represent the bow shock and magnetopause surfaces; they are conic sections (hyperbola and ellipse, respectively) fitted to the inbound and outbound bow shock and magnetopause crossings and constrained in shape to agree with gas dynamic analogs (4). The large tilt and offset of Neptune's magnetic field (3) produce a time-variable magnetic field configuration, resulting in periodic variations in the magnetospheric shape as the planet rotates. Comparison of the bow shock shape with those of the other planets shows that Neptune's bow shock is similar to Jupiter's and less flared than Earth's and Saturn's. The solar wind ion density, tem-

J. W. Belcher, H. S. Bridge, B. Coppi, G. S. Gordon, Jr., A. J. Lazarus, R. L. McNutt, Jr., J. D. Richardson, J. T. Steinberg, J. D. Sullivan, A. Szabo, L. Villanueva, M. Zhang, Massachusetts Institute of Technology, Cambridge, MA 02139.

F. Bagenal, University of Colorado, Boulder, CO 80309.
O. Divers, Jet Propulsion Laboratory, California Institute of Technology, Pasadena, CA 91109.

K. W. Ogilvie and E. C. Sittler, Jr., National Aeronautics and Space Administration Goddard Space Flight Center, Greenbelt, MD 20770.

G. L. Siscoe, University of California, Los Angeles, CA 90024.

A. Eviatar, Tel Aviv University, Tel Aviv, Israel.
V. M. Vasyliunas, Max-Planck-Institut für Aeronomie, Katlenburg-Lindau, Federal Republic of Germany.

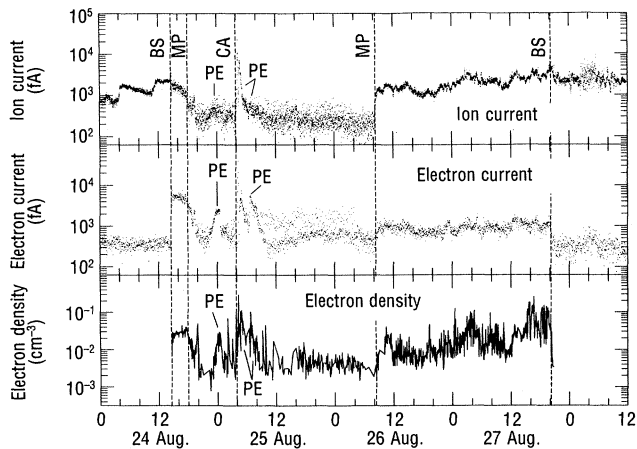


Fig. 1. Profiles of ion (top) and electron (middle) current (energy range, 10 eV to 1 keV for ions and 10 to 140 eV for electrons) and electron density (bottom) observed by the PLS experiment near Neptune. The current is in femtoamperes (10^{-15} A). Ion currents are from the C sensor. The bow shock (BS), magnetopause (MP), plasma enhancement (PE), and closest approach (CA) locations are labeled.

perature, and flow speed upstream from the first bow shock crossing were 0.0045 cm^{-3} , 0.5 eV, and 403 km s^{-1} , respectively. The solar wind ram pressure upstream from the magnetosphere was $1.2 \times 10^{-11} \text{ dyne cm}^{-2}$, and the magnetosonic Mach number upstream of the bow shock was about 6, much smaller than at Uranus (5). Because the bow shock crossing occurred at $34.3 R_N$ and nearly directly upstream from the planet, pressure balance alone implies a planetary dipole moment of 0.14 to $0.19 \text{ G} \cdot R_N^3$ in reasonable agreement with the value of $0.133 \text{ G} \cdot R_N^3$ derived from the MAG data (3). The plasma measurements show some small-scale structure associated with the bow shock but do not exhibit the large-amplitude oscillations observed behind Uranus's day-side bow shock (5).

Cusp region. We would have predicted a magnetopause crossing near $26 R_N$ on the basis of the bow shock location at $34.3 R_N$ and empirical scaling laws derived with observations at other planets. The magnetopause crossing was expected to be a very sharp boundary between the high fluxes of shocked solar wind plasma in the magnetosheath and the tenuous plasma that populates the outer magnetosphere. No sharp boundary was observed (Fig. 1). On 24 August at 1800 hours (all times are spacecraft event times), $26 R_N$ from Neptune, the electron and ion fluxes began to slowly decrease. The magnetosheath plasma finally disappeared at 1940 hours on 24 August, $23 R_N$ from the planet. The signal from the side-looking D sensor suddenly increased from a low magnetosheath level to a persistent, though fluctuating, higher level as Voyager 2 crossed the expected magnetopause distance, $26 R_N$, at 1800 hours on 24 August (Fig. 3). Our preliminary conclusion from these data, since confirmed by the MAG measurements (3), was that Voyager approached the planet through the cusp and that the crossing of the magnetopause, defined as the boundary between the magneto-

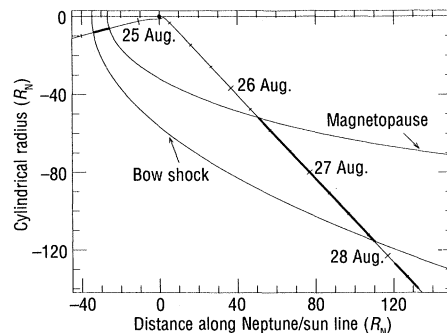


Fig. 2. Model bow shock and magnetopause for Neptune assuming axial symmetry about the Neptune/sun line. The surfaces are conic section approximations scaled to fit the crossings observed by the PLS experiment. The spacecraft trajectory is rotated about the symmetry axis into a meridional plane. Bold lines indicate where magnetosheath plasma was detected.

sheath and the cusp, did indeed occur at 1800 hours. During the subsequent 1 hour and 40 minutes, Voyager 2 transited the cusp region within the magnetosphere.

At Earth, the cusp regions always lie appreciably north and south of the nose of the magnetosphere, whereas Voyager 2 encountered the south polar cusp region of Neptune near the subsolar point. Although we recognize that these contrasting geometries may produce morphological differences in the terrestrial and Neptunian cases, it is nonetheless natural to think initially in terms of the terrestrial example. At Earth a cusp region comprises a turbulent entry layer and, tailward of this, a plasma mantle of coherent flow (6). Our preliminary survey of the plasma data shows aspects of both features, unsteady flow and unidirectional flow. Thus the data promise to add to our knowledge of comparative magnetospheres. However, further analysis incorporating the magnetic field data will be needed to determine the precise nature of Neptune's subsolar cusp region.

Plasma enhancements in the outer magnetosphere. Figure 4 shows an energy-time spec-

Table 1. Bow shock (BS) and magnetopause (MP) boundaries observed by the Voyager 2 PLS experiment.

Boundary	Time	Radial distance (R_N)	Distance from sun-planet line (R_N)
<i>Inbound pass</i>			
BS	24 Aug./14:38	34.8	8.3
MP	24 Aug./18:00	26.4	6.1
<i>Outbound pass</i>			
MP	26 Aug./08:19*	72.3	51.7
BS	26 Aug./20:27†	160.1	116.6
(out)			
BS	27 Aug./20:42†	161.6	117.1
(in)			
BS	27 Aug./21:05†	162.5	117.8
(out)			
BS	28 Aug./02:10	175.0	126.9
(in)			
BS	28 Aug./06:00‡	184.4	134.8
(out)			

*Transition lasted from ~ 0806 to ~ 0823 . †Times are approximate; crossings are not clearly defined in the data. ‡Wave activity associated with shock or multiple crossings to ~ 0900 .

rogram of data in the inner magnetosphere. From top to bottom are plots of high-energy (140 to 5950 eV) electrons, low-energy (10 to 140 eV) electrons, low-resolution ion data from the D sensor, and low-resolution ion data from the C sensor. In the outer magnetosphere, two significant enhancements of plasma flux occurred near 0000 and 0700 hours on 25 August, $11 R_N$ from Neptune inbound and $8.5 R_N$ from Neptune outbound, respectively. We tentatively identify these as plasma sheet crossings, although this interpretation is not yet definitive (in particular, the alternatives of a plasma torus confined in radial distance or longitudinal effects cannot be ruled out). The intensities of the ions and of the high- and low-energy electrons increase near the crossings. The ion increase is most evident in the D sensor, the detector looking in the corotation direction. The increased fluxes of hot electrons are centered approximately $0.5 R_N$ farther from the planet than those of the cold electrons at both plasma sheet crossings (compare panels E1 and E2 in Fig. 4). The local maxima in the ion fluxes occur closer to Neptune than either of the electron maxima. If the enhancements are indeed crossings of a plasma sheet confined near the magnetic equator, their locations at about 20° and 10°S (for the crossings at 0000 and 0700 hours on 25 August) must result from a large tilt of the planet's magnetic dipole from the planetary rotation axis; this conclusion agrees with the definitive results of the MAG experiments (3). Figure 5 shows the spacecraft trajectory in magnetic coordinates, based on the preliminary offset tilted

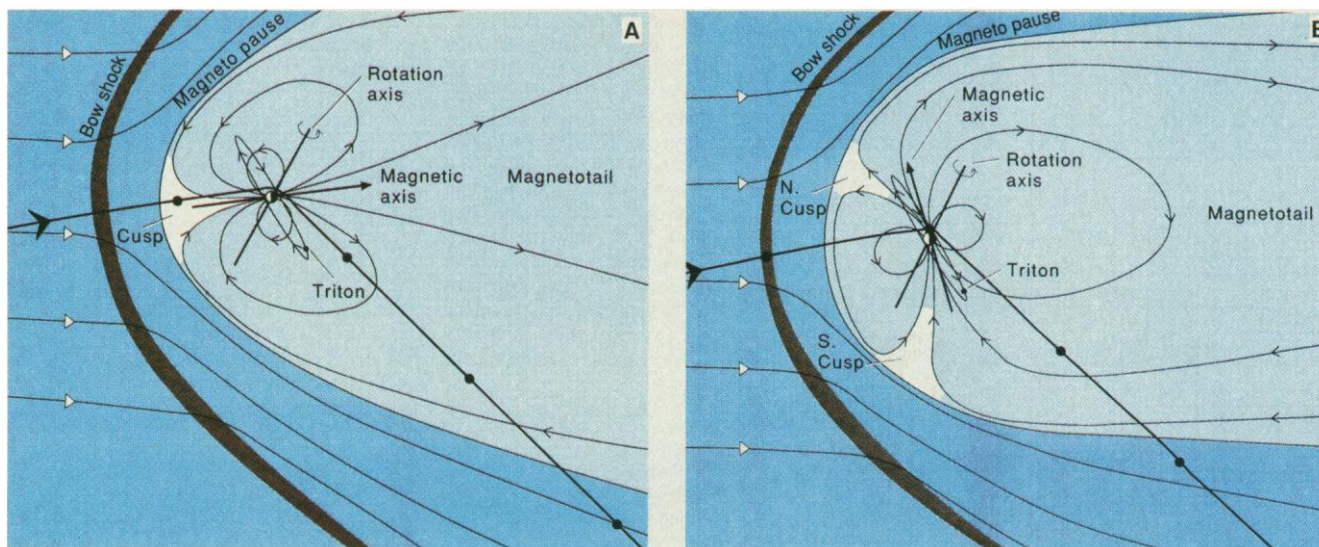


Fig. 3. Schematic drawings of a side view of the magnetospheric configuration at the time of the inbound magnetopause crossing (A) and half a primary rotation later (B). The solid dots on the spacecraft trajectory indicate

where Voyager was located each time the magnetosphere was in that configuration.

dipole (OTD) model of the magnetic field, which is a dipole tilted 46.8° from the rotation axis and offset from the center of the planet by $0.55 R_N$ (3). This model is considered to be a reasonable approximation between 4 and $15 R_N$ but is not valid closer to the planet where nondipolar terms are important (3). The crossings of the plasma sheet are not centered on the magnetic equator but are displaced slightly below it (Fig. 5) (this is not the direction of the offset expected from centrifugal effects).

Data from the D sensor show evidence of two ion components during both plasma sheet crossings. One energy-per-charge peak occurs between 10 and 30 V; the other is less intense and centered at about 200 V. Figure 6 shows a sample spectrum from the inbound plasma sheet crossing. The solid curves are best fits to the data, on the assumption that the two ion species are protons and N^+ , that the ion velocity distributions are convected isotropic Maxwellians, that the ions are corotating with Neptune, and that the spacecraft was not charged. The fit gives densities and temperatures of 0.07 cm^{-3} and 7 eV for the protons and 0.04 cm^{-3} and 65 eV for N^+ . These are fairly typical numbers for this region. Standard theory (7, 8) indicates that flow near Triton will deviate from corotation by more than 10% if $1 \times 10^3 \Sigma_p > M$, where Σ_p is the ionospheric conductivity in mho and M is the mass-loading rate in grams per second. A rough estimate of mass-loading from Triton resulting from sputtering of the atmosphere by a flux of $1 \times 10^4 \text{ cm}^{-2} \text{ s}^{-1}$ energetic protons (9) is 0.1 g s^{-1} , consistent with the pre-encounter prediction of a quiet magnetosphere (10). If the ionospheric conductivity is comparable to that at Saturn and

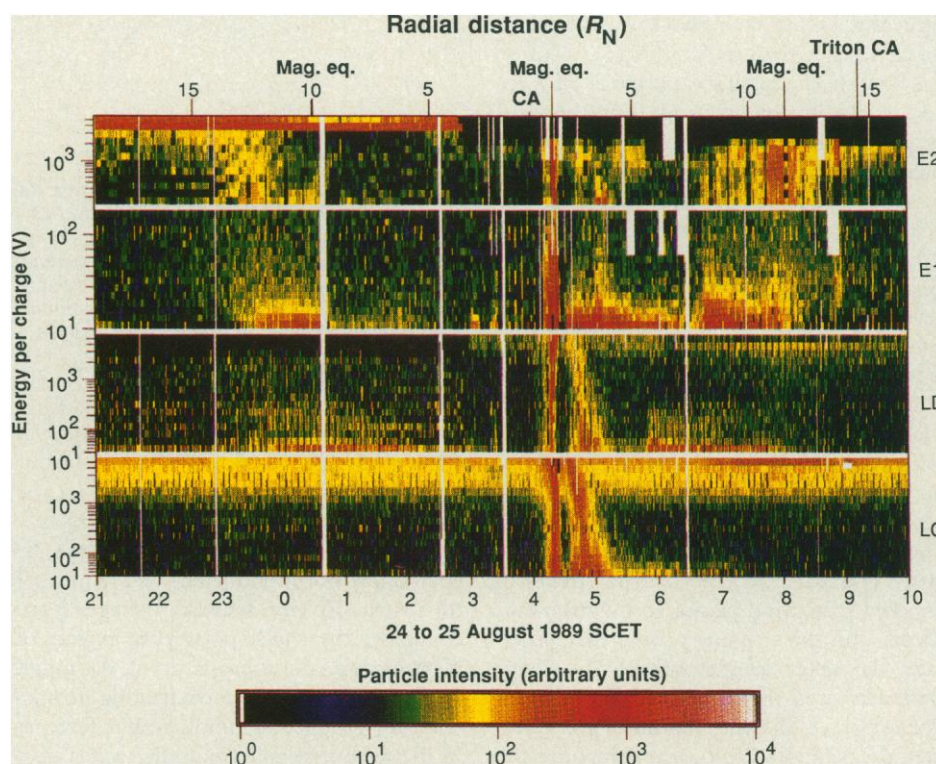


Fig. 4. Energy-time spectrograms of electron (top two panels) and ion (bottom two panels) intensities measured in the inner magnetosphere of Neptune. The ordinate is the energy per charge of the ions or electrons (equal to the energy for electrons and singly charged ions); SCET, spacecraft event time. In the upper (E2) and lower (E1) panels of electron data the logarithmic energy range spans 120 eV to 6 keV and 10 to 120 eV, respectively. The upper (LD) and lower (LC) panels of ion data comprise measurements made by the D and C sensors, respectively, and cover an energy-per-charge range of 10 to 5950 V. The bar at the bottom shows the key to the color scheme. White lines and rectangles are data gaps. Magnetic equator crossings and closest approaches to Neptune and Triton are labeled on the upper axis, as is radial distance from the center of the planet.

Uranus (on the order of 0.1 mho), then Neptune's ionosphere should be able to enforce corotation. The identification of the heavy ion as N^+ is not unique; other heavy ions (mass, 10 to 30) also give good fits to

the data. Data from the higher resolution M modes in this region are best fitted by ions heavier than protons (mass, 3 to 5) if rigid corotation and a spacecraft potential of 0 V are assumed. It is possible that the light ions

observed are He^+ , which would increase the mass of the heavy ions to 20 to 60. In this case a cold and possibly large proton component could be present at energies below our instrument threshold (10 V). An alternative explanation that we currently prefer is that a small negative spacecraft potential (on the order of 10 V) shifts the protons to higher energies so they appear to be heavier ions moving at the corotation speed. Electron densities and temperatures vary from about 0.002 cm^{-3} and 200 eV in the hot-electron enhancements to 0.1 cm^{-3} and 20 eV in the cold-electron enhancements. These densities are comparable to the ion densities and thus argue against a hidden proton population, unless we also postulate a comparable hidden cold-electron component. The plasma wave (PWS) experiment derives densities from upper hybrid resonance emissions that are in agreement with those observed by PLS, indicating that hidden populations are not present.

Closest approach. In addition to the two plasma sheet crossings in the outer magnetosphere described above, two density enhancements were observed near closest approach. The first, at 0420 hours on 25 August, is readily visible in the energy-time spectrogram (Fig. 4) in both the ion data and the high- and low-energy electron data. The plasma is hot in this region; the intense ion fluxes extend up to 6 kV. No distinct peaks corresponding to different ion species were observed; several ion species may be present, but, if so, the plasma was too hot to permit them to be resolved. Assuming all the ions are protons gives a total density of 0.6 cm^{-3} ; assuming the low-energy ions are protons and the high-energy ions are N^+ gives a density of 1.4 cm^{-3} . Thermal electron densities and temperatures are 0.3 cm^{-3} and 50 eV, respectively. This feature is near the magnetic equator predicted by the OTD magnetic field model; thus we interpret it as another plasma sheet crossing, although we are aware that this model is not valid this close to the planet (3).

The second enhancement close to the planet extended from 0440 to 0600 hours on 25 August. From 0440 to 0450 the ions were again hot, although the spectra were softer and the ion density was slightly less than those near 0420 hours. The electron temperature, however, was much lower, only 10 to 20 eV. The average ion energy decreased away from Neptune to a few tens of electron volts after 0510 hours. The electron temperature increased after 0440 hours to a peak at about 0510, then decreased out to 0620 hours. High-energy electrons were observed for a short period near 0510, just after the hot ions disappeared. The long duration of this flux en-

hancement in a region where the magnetic configuration is complicated (nondipolar) makes it unlikely that this is a simple plasma sheet crossing. The latitudinal extent of the plasma sheet may be large in this region so that the spacecraft remained within it as Voyager moved away from Neptune or this enhancement could be plasma trapped on closed field lines near the planet. The high plasma temperatures indicate that a latitudinally extended plasma sheet is possible, but this will also depend on the temperature anisotropy, which is not yet known. It is possible that ion spectra are softer in this region than at 0420 hours because the population of heavy ions, which have higher energies, would decrease more rapidly than protons away from the equator. Because the magnetic latitude changes rapidly in this region, detailed knowledge of the planetary magnetic field will be needed to interpret these data properly.

Close to the planet the loss cones are very large, up to 40° at closest approach, so that densities may be over- or underestimated depending on the orientation of the detector to the magnetic field. No evidence of field-aligned streaming of either ions or electrons is present in the PLS data. The low-energy charged particle (LECP) experiment reports evidence of the field-aligned electron flow near closest approach (9). No signature is apparent in the PLS electron channels at this time, although the detector was properly oriented to detect downstreaming electrons. Failure to observe downstreaming electrons could indicate that a field-aligned potential drop above the spacecraft accelerated these electrons above 6 kV, the highest energy per charge detectable by our instrument, or that electron fluxes were below our instrument threshold.

Downstream region. As Voyager moved from the outbound magnetopause crossing through the magnetosheath to the bow shock, the plasma density in the magnetosheath increased from 0.001 to 0.004 cm^{-3}

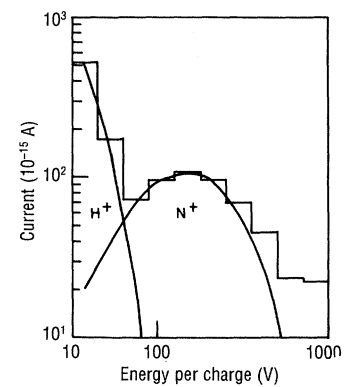


Fig. 6. Ion L mode spectrum from the first plasma sheet crossing taken at 0018 hours on 25 August. Measured current from the D sensor is plotted versus energy. The curves show the best fit to the data obtained for two ion species, protons and N^+ , which have convected isotropic Maxwellian velocity distributions and corotate with the planet.

and the velocity increased from 300 to 380 km s^{-1} . These results are consistent with variations predicted by magnetogasdynamic theory (11). Superimposed on the gradual increase in velocity and density are large (factor of 2 to 5) enhancements of plasma density with periods of tens of minutes. These enhancements are anticorrelated with changes in plasma temperature and are associated with changes in the plasma flow direction. Similar density fluctuations were observed at Uranus and are probably associated with the downstream shock (12). Longer period oscillations in the plasma density and flow velocity with a period of 8 hours (half a planetary rotation) may also be present in the magnetosheath. These variations may reflect changes in the shape of the magnetosphere as the planet rotates, but further study is needed before firm conclusions can be drawn. Large-amplitude, low-frequency waves were observed in the solar wind starting at 0730 hours on 29 August. Although comparisons with magnetic field observations have yet to be performed, at

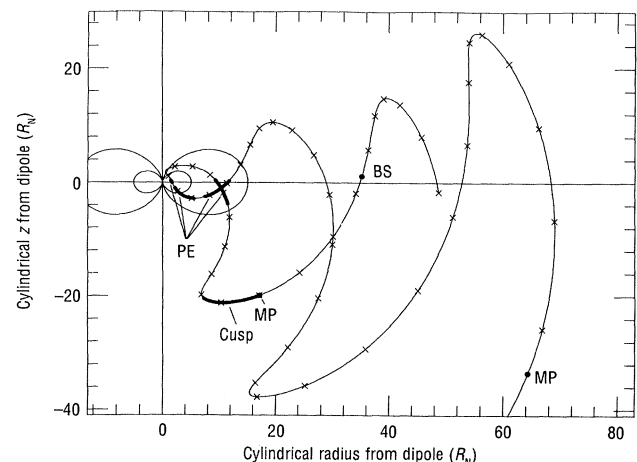


Fig. 5. Trajectory of the spacecraft in magnetic coordinates corresponding to the offset, tilted dipole magnetic field model (3). The bow shock (BS), magnetopause (MP), cusp, and plasma enhancements in the outer magnetosphere and near closest approach (PE) are labeled.

Uranus this signature indicated the presence of magnetohydrodynamic waves that were probably generated by energetic particles streaming away from the bow shock.

Magnetospheric configurations. The general configuration and dynamics of a magnetosphere are governed by two angles: (i) the angle between the planet's rotation axis and its magnetic axis and (ii) the angle between the rotation axis and the direction of the solar wind. The larger the tilt of the magnetic dipole, the more the magnetospheric configuration changes over a planetary rotation period. If the rotation axis is roughly normal to the solar wind direction, then the convective motion of the magnetospheric plasma can either be dominated by rotation (as at Jupiter and Saturn and in Earth's plasma-sphere) or driven by the solar wind (as in most of Earth's magnetosphere). When the rotation axis lies close to the solar wind direction (as at Uranus), corotation and the solar wind-driven convection are orthogonal and both types of motion can occur simultaneously (13). Neptune's rotation axis is 70° from the solar wind direction, and one expects a corotation-dominated magnetosphere similar to those of Jupiter and Saturn (14, 15). The large tilt of Neptune's dipole from its rotation axis should result in strong longitudinal asymmetries and temporal variations due to changes in the configuration of the magnetosphere as Neptune rotates (such as those sketched in Fig. 3). Specifically, the shape of the magnetopause, the location of the cusp regions, and the reconnection geometry of the planetary and interplanetary magnetic fields change considerably over Neptune's 16-hour rotation period. Once every 16 hours, the southern magnetic pole points directly into the solar wind, producing a large cusp on the dayside magnetopause while the northern magnetic pole points down the magnetotail (Fig. 3A). Half a rotation later, Neptune's magnetosphere reverts to a more Earth-like configuration (Fig. 3B).

Plasma sources and transport. The observations described here enable us to draw some tentative conclusions regarding the origin and transport of the magnetospheric plasma. Possible magnetospheric plasma sources are the solar wind, Triton, the inner moons and rings, and Neptune itself. The solar wind is probably not an important source because little He^{2+} , a characteristic solar wind ion, was detected by the LECP instrument (9). In addition, entry of solar wind plasma into Neptune's inner magnetosphere is difficult because the plasma must be transported inward by relatively slow diffusive processes.

Triton has an atmosphere and a dense ionosphere (16) and should be a plasma source via direct ionospheric escape and

sputtering of the atmosphere by ions and solar radiation. Pre-encounter calculations predicted that a torus of heavy ions would surround Triton, with plasma densities of 0.04 to 8 cm^{-3} (17). The observations show that heavy ion densities are at the lower limit of this range, about 0.04 cm^{-3} , and that the heavy ions are only observed at the plasma sheet crossings, not at Triton's orbit. Despite this discrepancy in location, the source of the heavy ions may still be Triton. The inferred ion mass is consistent with nitrogen ions, and the temperature, 60 to 100 eV, is consistent with the 120-eV pickup energy at Triton's minimum L shell (the smallest L shell intersected by Triton's orbit). The observed density of heavy ions in the outer plasma sheet crossings agrees quite well with the predicted Triton torus values because the energetic particle flux measured by the LECP instrument (about $10^4 \text{ cm}^{-2} \text{ s}^{-1}$), is near the flux that yielded the lower predicted densities. The tilt of the magnetic dipole results in a geometry in which the torus of neutrals surrounding Triton's orbit intersects Triton's minimum L shell at only two longitudes, 170° and 350° ; this effect may produce a plasma torus that has strong longitudinal asymmetries.

The inner moons and rings of Neptune are very dark, similar to those at Uranus. Radiation darkening is probably responsible; this process forms a tarlike material that has low sputtering yields (18), so these bodies are probably not major plasma sources. Escape from Neptune's atmosphere and ionosphere is probably the major mode of escape of magnetospheric protons. The exospheric temperatures at Neptune are much lower than at Uranus, so the source rates are less than at Uranus. Neptune has no equivalent to the large H corona, which provided an important plasma source at Uranus. Possible escape mechanisms for protons from the ionosphere include a polar wind and upward acceleration by auroral electric fields.

The ions in the outer plasma sheet crossings have temperatures near the local pickup energy, 7 eV for protons and 120 eV for N^+ . It seems likely that this plasma is produced locally near Triton, consistent with a Triton source. Although the pickup energy near closest approach is less than 0.1 eV, the plasma in this region has temperatures of tens to hundreds of electron volts. The simplest heating mechanism is to transport this material inward from the outer plasma sheet. Conservation of the first adiabatic invariant requires that $T_\perp \propto B$ (T_\perp is the temperature of particles moving perpendicular to the field lines), and, since $B \propto L^{-3}$ [for a dipole magnetic field B the dependence will be stronger close to Neptune

where the field has nondipolar components (3)], plasma transported from $L = 10$ to $L = 2$ will gain at least a factor of 100 in energy, easily sufficient to account for the observed temperatures. Compression of the magnetic field toward the planet causes the density to increase inward at least as rapidly as $1/L^3$ as a result of the decrease in volume of a magnetic flux tube. Thus a plasma sheet density of 0.1 cm^{-3} at $L = 10$ would increase to over 10 cm^{-3} at $L = 2$. Loss processes, such as precipitation of ions into the atmosphere, may keep the actual density down to the 1 cm^{-3} observed.

In summary, we find that Neptune has a magnetosphere with a very dynamic configuration resulting from the large dipole tilt. The magnetospheric plasma densities are very low, mainly due to a paucity of plasma sources. Neptune's atmosphere is too cold to be a major source of neutral species. The surfaces of the inner moons and rings are probably irradiated into complex compounds, from which ejection into the magnetosphere is difficult. Solar wind plasma cannot easily penetrate into the inner magnetosphere. Triton, a likely source, is hampered by the large dipole tilt, which increases the volume it must fill with plasma, by the relatively low flux of energetic particles, and by its low atmospheric temperature, which results in low escape rates.

REFERENCES AND NOTES

1. H. S. Bridge, *Space Sci. Rev.* **21**, 259 (1977).
2. E. C. Sittler, Jr., K. W. Ogilvie, R. S. Selesnick, *J. Geophys. Res.* **92**, 15,263 (1987).
3. N. F. Ness et al., *Science* **246**, 1473 (1989).
4. J. A. Slavin et al., *J. Geophys. Res.* **90**, 6275 (1985).
5. F. Bagenal et al., *ibid.* **92**, 8603 (1987).
6. G. Haerendel et al., *ibid.* **83**, 3195 (1978).
7. D. H. Pontius and T. W. Hill, *Geophys. Res. Lett.* **12**, 1321 (1982).
8. A. Eviatar et al., *J. Geophys. Res.* **88**, 823 (1983).
9. S. M. Krimigis et al., *Science* **246**, 1483 (1989).
10. A. J. Dessler and B. R. Sandel, *Geophys. Res. Lett.* **16**, 957 (1989).
11. J. R. Spreiter, *ibid.* **85**, 6769 (1980).
12. J. D. Richardson et al., *ibid.*, in press.
13. V. M. Vasyliunas, *Geophys. Res. Lett.* **13**, 621 (1986).
14. G. L. Siscoe, in *Solar System Plasma Physics*, vol. 2, C. F. Kennel, L. J. Lanzerotti, E. N. Parker, Eds. (North-Holland, Amsterdam, 1978), pp. 319-402.
15. R. S. Selesnick and J. D. Richardson, *Geophys. Res. Lett.* **13**, 624 (1986).
16. G. L. Tyler et al., *Science* **246**, 1466 (1989).
17. M. L. Delitsky, A. Eviatar, J. D. Richardson, *Geophys. Res. Lett.* **16**, 215 (1989).
18. L. J. Lanzerotti, *J. Geophys. Res.* **92**, 14,949 (1987).
19. We thank our colleagues on the PLS team, P. Milligan, J. Quigley, and A. Bowes, for their help preparing for and during encounter. We thank the entire Voyager Project staff for their support, which made our experiment, and the entire mission, a success. We also thank W. Mish, T. Carleton, R. Kennon, T. Vollmer, L. Moriarty, S. Kempler, and F. Ottens at the Laboratory for Extraterrestrial Physics and P. Harrison, J. Jones, and S. Kramer at STX for assistance with the data analysis. P. Liggett, L. Lee, S. Burlleigh, and the entire VNESSA staff at the Jet Propulsion Laboratory provided invaluable assistance in displaying the real time data. We appreciated discussions and information from the

Hot Plasma and Energetic Particles in Neptune's Magnetosphere

S. M. KRIMIGIS, T. P. ARMSTRONG, W. I. AXFORD, C. O. BOSTROM, A. F. CHENG, G. GLOECKLER, D. C. HAMILTON, E. P. KEATH, L. J. LANZEROTTI, B. H. MAUK, J. A. VAN ALLEN

The low-energy charged particle (LECP) instrument on Voyager 2 measured within the magnetosphere of Neptune energetic electrons (22 kiloelectron volts $\leq E \leq 20$ megaelectron volts) and ions (28 keV $\leq E \leq 150$ MeV) in several energy channels, including compositional information at higher (≥ 0.5 MeV per nucleon) energies, using an array of solid-state detectors in various configurations. The results obtained so far may be summarized as follows: (i) A variety of intensity, spectral, and anisotropy features suggest that the satellite Triton is important in controlling the outer regions of the Neptunian magnetosphere. These features include the absence of higher energy (≥ 150 keV) ions or electrons outside $14.4 R_N$ (where R_N = radius of Neptune), a relative peak in the spectral index of low-energy electrons at Triton's radial distance, and a change of the proton spectrum from a power law with $\gamma \geq 3.8$ outside, to a hot Maxwellian ($kT \approx 55$ keV) inside the satellite's orbit. (ii) Intensities decrease sharply at all energies near the time of closest approach, the decreases being most extended in time at the highest energies, reminiscent of a spacecraft's traversal of Earth's polar regions at low altitudes; simultaneously, several spikes of spectrally soft electrons and protons were seen (power input $\approx 5 \times 10^{-4}$ ergs $\text{cm}^{-2} \text{s}^{-1}$) suggestive of auroral processes at Neptune. (iii) Composition measurements revealed the presence of H, H₂, and He⁴, with relative abundances of 1300:1:0.1, suggesting a Neptunian ionospheric source for the trapped particle population. (iv) Plasma pressures at $E \geq 28$ keV are maximum at the magnetic equator with $\beta \approx 0.2$, suggestive of a relatively empty magnetosphere, similar to that of Uranus. (v) A potential signature of satellite 1989N1 was seen, both inbound and outbound; other possible signatures of the moons and rings are evident in the data but cannot be positively identified in the absence of an accurate magnetic-field model close to the planet. Other results include the absence of upstream ion increases or energetic neutrals [particle intensity (j) $< 2.8 \times 10^{-3} \text{ cm}^{-2} \text{ s}^{-1} \text{ keV}^{-1}$ near 35 keV, at $\sim 40 R_N$] implying an upper limit to the volume-averaged atomic H density at $R \leq 6 R_N$ of $\leq 20 \text{ cm}^{-3}$; and an estimate of the rate of darkening of methane ice at the location of 1989N1 ranging from $\sim 10^5$ years (1-micrometer depth) to $\sim 2 \times 10^6$ years (10-micrometers depth). Finally, the electron fluxes at the orbit of Triton represent a power input of $\sim 10^9$ W into its atmosphere, apparently accounting for the observed ultraviolet auroral emission; by contrast, the precipitating electron (> 22 keV) input on Neptune is $\sim 3 \times 10^7$ W, surprisingly small when compared to energy input into the atmosphere of Jupiter, Saturn, and Uranus.

THE PRIMARY SCIENTIFIC OBJECTIVES of the LECP investigation during the encounter of Voyager 2 with Neptune were to discover the nature of the planet's magnetosphere (if any), to measure the intensity, energy spectra, composition, angular distributions, and spatial and temporal characteristics of magnetospheric ions ($E \geq 28$ keV) and electrons ($E \geq 22$ keV), and to determine the nature and importance of the interactions of these particle populations with Triton and with the subsequently discovered Neptunian satellites N1-N6, as

well as the planetary rings. The LECP instrument has two sensor systems: the low-energy particle telescope (LEPT) and the low-energy magnetospheric particle analyzer (LEMPA), both of which have a large number of solid-state detectors that can be used in various coincidence-anticoincidence configurations. In order to obtain angular distributions, the detector heads are mounted on a platform that rotates through 360° on the three axis-oriented Voyager spacecraft. One of the angular positions places the sensors behind a 2-mm-thick aluminum

shield to obtain an accurate measure of background. Because of several spacecraft constraints during the Neptune encounter, the detector heads were kept stationary either in sector 1 or sector 7, with the exception of periodic (every 6 min) 360° scans of 48 s or 96 s in duration. These periodic scans were interrupted during inbound and outbound crossings of the planetary equatorial plane so that the instrument's sensitive detectors would be protected from the impact of micron-sized particles co-orbiting with the planet. Continuous, 360° scans of the instrument, one scan per 6.4 min, were used 12 hours before the closest approach and resumed ~ 24 hours after periapsis. A full description of the LECP instrument is contained elsewhere (1).

Overview. The Voyager discovery of the magnetosphere of Neptune, as recorded by the LECP instrument, is summarized in Fig. 1, which shows a color spectrogram as a function of spacecraft event time (SCET) of the intensities of ions and electrons for a 2-day period beginning on 24 August (day 236) at 1400 SCET. Before the inbound bow shock (BS) crossing, there was no hint of upstream ion activity, the first planet encountered by Voyager where this was the case (2). The absence at Neptune of clear, BS-associated proton and electron enhancements is also an unusual aspect of planetary magnetosphere encounters by Voyager. Further, there was only a modest increase in the proton intensities at the magnetopause (MP) and a marginal electron intensity increase, both of which are unique in the context of planetary magnetospheres investigated by Voyager. Only low-energy (≤ 150 keV) protons and electrons were present outside the radial location of Triton, and there were rapid increases in the intensities of higher energy particles inside that satellite's orbit (Fig. 1). A clear dip in the intensity of low-energy protons near the radial location of Triton is evident, both inbound and outbound. The peak intensity of the lowest energy electrons occurs at ~ 2330 SCET on 24 August, substantially earlier than the intensity peak for either the high-energy electrons (~ 0100 SCET) or the protons at any energy. Additional peaks in the lowest energy electron intensities oc-

S. M. Krimigis, C. O. Bostrom, A. F. Cheng, E. P. Keath, B. H. Mauk, Applied Physics Laboratory, The Johns Hopkins University, Laurel, MD 20707-6099.

T. P. Armstrong, the University of Kansas, Lawrence, KS 66044.

W. I. Axford, Max-Planck-Institut für Aeronomie, Postfach 60, 3411 Lindau, Federal Republic of Germany.

G. Gloeckler and D. C. Hamilton, University of Maryland, College Park, MD 20742.

L. J. Lanzerotti, AT&T Bell Laboratories, Murray Hill, NJ 07974.

J. A. Van Allen, University of Iowa, Iowa City, IA 52242.